Virial Coefficients of Ethane from a Quadrupolar Site-Site Potential Function

[a]Kenneth O. Monago and [b]Charles Otobrise

[a]Department of Pure and Industrial Chemistry, University of Port -Harcourt, Port-Harcourt, Nigeria.

[b]Department of Chemistry, Delta State University, Abraka, Nigeria.

[b]E-mail: otobrisec@delsu.edu.ng

ABSTRACT

A procedure based on a site-site pair potential function, combined with the triple-dipole term, was used to determine the second and third virial coefficients of linear ethane. The parameters in the two-body potential were determined in a fit to experimental second acoustic virial coefficients; no other data were used. The three-body strength coefficient was determined in a fit to speed-of-sound data using isotropic two-body and three-body potentials. The resulting potential parameters reproduced second acoustic virial coefficients and predicted second volumetric virial coefficients of ethane to within an absolute error of 0.5 cm^3 mol^{-1}. The third volumetric virial coefficients were predicted to within an absolute error of 250 cm^6 mol^{-2}. Third acoustic virial coefficients of ethane predicted with the procedure are in good agreement with experiment only at temperatures above about 240 K; below this temperature the two sets of values are inconsistent.

1. INTRODUCTION

Following the enumeration and computation of three-body graphs in the fourth virial coefficient, it is now known that a fourth-order virial equation of state, far from being a low-density expansion can predict P-V-T properties of gases with high accuracy up to one-half the critical density, or in terms of pressure up to 12 MPa (Monago, 2005; Monago, 2013; Monago 2010, and Wiebke et al., 2011). At present, our only source of fourth virial coefficient is by computation, because it is difficult to extract its valuesfrom experimental volumetric data. The only experimental fourth virial coefficient datathat are known to the author and of which there is corroborative evidence of their accuracy are those of Estrada-Alexanders (Estrada-Alexanders, 1996).
For real molecular fluids, calculation of virial coefficients have been limited largely at the

second virial coefficient level (Estrada-Alexanders, 1996; Ewing and Trusler, 1992; Estela-Uribe and Trusler, 2000, andMeng and Duaa, 2006);however, there are a few published works on third virial coefficient: Lucas and his co-workers used an anisotropic potential function to calculate the third virial coefficients of some linear molecules. Ameling and Lucas, (1986); Ameling et al., (1986) and Kusalik et al., (1995); have calculated the third virial coefficients of certain non-linear water models. Benjamin et al., (2009) andShaul et al., (2011); have calculated virial coefficients up to the fifth order using Monte Carlo sampling methods. However, no experimental data exist with which to verify the accuracies of volumetric coefficients higher than the third; and it would appear that virial coefficients calculated by these methods are not yet sufficiently accurate. For example, second and third virial

coefficients calculatedby Kim et al., (2013) for mixtures of methane and ethane disagreed with experiment by between 5 – 10 percent and 20 – 30 percent, respectively. Also, pressure calculated by Benjamin et al., (2009) using virial coefficients up to the fifth order was deemed accurate only up to $\rho_c/2$.

The purpose of this paper is to use a site-site pair potential function with a point quadrupole to calculate the first two virial coefficients(and their first two temperature derivatives) of molecular ethane and to compare the results obtained here with experimental data.

2. THEORETICAL FRAMEWORK

The relationship between an angle-dependent potential function and second volumetric virial coefficient, B, is:

$$B = -\frac{N_A}{4} \int_0^\infty r_{12}^2 \, dr_{12} \int_{-1}^1 d(cos\theta_1) \int_{-1}^1 d(cos\theta_2) \int_0^{2\pi} f_{12} \, d\varphi_{12} \qquad [1]$$

The analogous expression for third volumetric virial coefficient, C, is:

$$C = -\frac{N_A^2}{24\pi} \int_0^\infty r_{12}^2 \, dr_{12} \int_0^\infty r_{13}^2 \, dr_{13} \int_{-1}^1 d(cos\alpha) \int_{(\theta)} \int_{(\varphi)} (f_{12}f_{13}f_{23} + e_{12}e_{13}e_{23}f_{123}) \, d\acute{\theta}d\acute{\varphi} \quad [2]$$

Where,

$$\int_{(\theta)} = \int_{-1}^1 d(cos\acute{\theta}_1) \int_{-1}^1 d(cos\acute{\theta}_2) \int_{-1}^1 d(cos\acute{\theta}_3), \quad \int_{(\varphi)} = \int_0^{2\pi} d\acute{\phi}_1 \int_0^{2\pi} d\acute{\phi}_2 \int_0^{2\pi} d\acute{\phi}_3 \text{ and}$$

$$cos\alpha = \mathbf{r}_{12} \cdot \mathbf{r}_{13}/r_{12}r_{13}.$$

The other symbols have their usual meanings. Eq. (1) and (2) are written in the space-fixed reference frame and the notations in the above expressions follow those used by Lucas (1991).
The systems we consider in this article are composed of symmetric linear molecules between which there exist both pairwise as well as non-additive three-body forces. These forces can be specified by a pair potential function, $\phi(r_{12},\omega_1,\omega_2)$ and triplet potential function $\Delta\phi_{123}$. In this work, pairwise forces are modelled by the two-center Maitland-Smith potential function with a point quadrupole.

$$\emptyset(r_{12}, \omega_1\omega_2) = \frac{1}{4}\sum_{j=1}^2 \sum_{i=1}^2 \frac{\varepsilon}{n-6}\left\{6\left(\frac{r_m}{r_{ij}}\right)^n - n\left(\frac{r_m}{r_{ij}}\right)^6\right\} + \emptyset_{QQ} \qquad [3]$$

Where, $n = m + \tau\left\{\left(\frac{r_{ij}}{\sigma}\right) - 1\right\}$, and

$$\emptyset_{QQ} = \frac{3\Theta^2}{4r_{12}^5}\{1 - 5(c_1^2 + c_2^2 + 3c_1^2c_2^2) + 2(s_1s_2c_{12} - 4c_1c_2)^2\} \qquad [4]$$

In the above scheme, ω_i denotes the orientation angle of moleculei, $C_i = \cos\theta_i$, $S_i = \sin\theta_i$, r_{ij} is the distance between site i in one molecule and site j in another and r_{12} is the center-to-center distance between two molecules; also, Θ is the quadrupole moment of ethane. For the system under consideration, r_{12} and r_{ij} are related by Eq. (5) (Lucas, 1991).

$$r_{ij}^2 = r_{12}^2 + l_1^2 + l_2^2 - 2r_{12}[(\pm l_1)c_1 - (\pm l_2)c_2] - 2(\pm l_1)(\pm l_2)[c_1c_2 + s_1s_2c_{12}] \; [5]$$

Where, l_i is the distance of site i from the center of mass of the molecule and $C_{12}=$ $Cos\varphi_{12}$. For the interactions between only two molecules, one may choose the center-to-center distance to lie along the z-axis in the space-fixed frame; therefore, Eq. (4) and (5) may be used with Eq. (1) without modification. However, for the interactions between three molecules, one must relate the general angles,(θ,φ), to the angles in the intermolecular reference frame,(θ,φ). Details of this transformation are given in (Ameling et al., 1986 and Lucas, 1991). Lucas (1991) in particular gives the relationships between the two sets of angles for the interactions between molecule1 and 3. For those between molecules 1 and 2, the appropriate relationships are:

$$cos\theta = sin\acute{\theta}cos\,(\acute{\phi} - \alpha)$$

$$sin\varphi = \frac{sin\theta sin\acute{\phi} - sin\alpha cos\theta}{cos\alpha sin\theta}$$

$$cos\varphi = -cos\acute{\theta}/sin\theta$$

For interactions between molecules 2 and 3, the relevant relationships are:

$$cos\theta = sin\acute{\theta}cos\,(\acute{\phi} + \gamma)$$

$$sin\varphi = \frac{sin\acute{\theta}sin\acute{\phi} + sin\gamma cos\theta}{cos\gamma sin\theta}$$

$$cos\varphi = -cos\acute{\theta}/sin\theta$$

Where, $cos\xi = \mathbf{r}_{13} \cdot \mathbf{r}_{23}/r_{13}r_{23}$. In computing third virial coefficient, non-additive forces were modelled by the Axilrod-Teller triple dipole term:

$$\Delta\emptyset(r_{123}) = \frac{3\vartheta_{123}}{8(r_{12}r_{13}r_{23})^3}\left\{\frac{2}{3} + \frac{r_{12}^2+r_{13}^2}{r_{23}^2} + \frac{r_{12}^2+r_{23}^2}{r_{13}^2} + \frac{r_{13}^2+r_{23}^2}{r_{12}^2} - \frac{r_{12}^6+r_{13}^6+r_{23}^6}{(r_{12}r_{13}r_{23})^2}\right\}$$

[6]

In Eq. (6), ϑ_{123} is the three-body strength coefficient, which adds the fifth parameter to the overall model. Since we are here dealing with symmetric linear molecules, Eq. (2) was re-written as:

$$C = -\frac{N_A^2}{12\pi}\int_0^\infty r_{12}\,dr_{12}\int_{r_{12}/2}^\infty r_{13}\,dr_{13}\int_{|r_{12}-r_{13}|}^{r_{13}}r_{23}\,dr_{23}\int_{(\theta)}\int_{(\varphi)}(f_{12}f_{13}f_{23} + e_{12}e_{13}e_{23}f_{123})\,d\acute{\theta}d\acute{\phi}$$

[7]

The first two temperature derivatives of B and C were obtained by ordinary differentiation of Eq. (1) and (7) (Monago, 2005).

3. NUMERICAL METHODS

The virial coefficients were calculated according to eq. (1) and (7), using multi-panel Gaussian quadrature. In the case of B, the semi-infinite integration over r_{12} was performed as follows: first, the interval (0, r_{max}) was divided into three panels jointed at $r_{12} = 2\sigma$ and $r_{max} = 20\sigma$. The first and second panels were further sub-divided into 6 and 12 equal partitions, respectively, and each partition was integrated over by a 5 point Gaussian quadrature. The last panel was integrated over analytically. In the case of C, integration over r_{12} was performed as for B, except that the interval (0, r_{max}) was divided into two panels jointed at $r_{12} = 2\sigma$. The range in this case was to a maximum distance (r_{max}) of 8σ. The first panel was sub-divided into 6 equal partitions, while the second was sub-divided into 5 partitions; in

both cases each partition was integrated over by a 3 point Gaussian quadrature.

In eq. (7), the lower limit of integration over r_{13} depends on r_{12}, whereas the limits over r_{23} depend on both r_{13} and r_{12}. Integration over r_{13} and r_{23} were performed such that if the panel lay in the range (0, 2σ), it was divided into N_1 equal partitions such that $2\sigma/N_1 \approx \sigma/3$. Conversely, when the panel lay in the range (2σ, r_{max}), it was divided into N_2 partitions such that $(r_{max} - 2\sigma)/N_2 \approx \sigma$. Each partition was then integrated over by a three-point Gaussian quadrature.

For both B and C, angle integration over $cos\dot{\theta}_i$ was performed with the interval (0, π/2) divided into two equal partitions; each partition being integrated over by a three-point Gaussian quadrature. The reduction in the range of integration was possible because of the symmetry in $cos\dot{\theta}_i$. Similarly, for integration over $\dot{\phi}_i$ and $\dot{\phi}_{i,j}$, use was made of the symmetry about π and the interval (0, π) was divided into four equal partitions; thereafter, each partition was integrated over with a three-point Gaussian quadrature.

The first two temperature derivatives of B and C were calculated by quadrature, as the virial coefficients themselves (Monago, 2013). Second, β, and third, γ, acoustic virial coefficients were calculated from B, C, their two temperature derivatives and the heat capacity of ethane in the hypothetical perfect-gas state (Estrada-Alexanders, 1996 and Ewing and Trusler, 1992) and as shown below in Eq. (8) and (9)

$$\beta = 2B + 2\left(\gamma_{pg} - 1\right)TB^{(1)} + \frac{\left[T\left(\gamma_{pg}-1\right)\right]^2 B^{(2)}}{\gamma_{pg}}. \tag{8}$$

$$\gamma = \frac{\gamma_{pg}-1}{\gamma_{pg}}\left[B + \left(2\gamma_{pg} - 1\right)TB^{(1)} + \left(\gamma_{pg} - 1\right)T^2 B^{(2)}\right]^2 +$$

$$\frac{2\left(2\gamma_{pg}+1\right)C + 2\left(\gamma_{pg}^2-1\right)TC^{(1)} + \left(\gamma_{pg}-1\right)^2 T^2 C^{(2)}}{2\gamma_{pg}}. \tag{9}$$

Where, in Eq. (8) and (9), $B^{(1)}$ and $B^{(2)}$ are, respectively, the first and second temperature derivatives of B; $C^{(1)}$ and $C^{(2)}$ are similarly defined. Also, $\gamma_{pg} = C_P^{pg}/C_v^{pg}$, is the ratio of the two heat capacity functions of ethane in the perfect-gas state. In the case of B and its derivatives, all first-order quantum corrections, including the coriolis term, were included in the calculations (Pack, 1983). Quantum corrections to B were implemented as follows:

$$B = B_{class} = \frac{\hbar^2}{\mu}B_{t1} + \frac{\hbar^2}{I}B_{r1} + \frac{\hbar^2}{\mu}B_c \tag{10}$$

In Eq. (10), B_{class} is the classical ordinary second virial coefficient, Eq. (1); μ is the reduced mass and I is the moment of inertia of the molecule. The coefficients B_{t1}, B_{r1} and B_c determine, respectively, the first-order translational, rotational and coriolis contributions to the quantum corrections. For a system composed of identical molecules, the coefficients are defined as follows:

$$B_{t1} = \frac{N_A}{96(kT)^3}\int_0^\infty \int_\Omega e(r)\left(\frac{\partial \emptyset}{\partial r_{12}}\right)^2 r_{12}^2 \, d\Omega dr_{12}$$

$$B_{r1} = \frac{N_A}{96(kT)^3}\int_0^\infty \int_\Omega e(r)\left\{\left(\frac{\partial \emptyset}{\partial \theta_1}\right)^2 + \left(\frac{\partial \emptyset}{\partial \theta_2}\right)^2 + S_1^{-2}\left(\frac{\partial \emptyset}{\partial \varphi_1}\right)^2 + S_2^{-2}\left(\frac{\partial \emptyset}{\partial \varphi_2}\right)^2\right\} r_{12}^2 \, d\Omega dr_{12}$$

$$B_c = \frac{N_A}{96(kT)^3} \int_0^\infty \int_\Omega e(r) F(r_{12}, \theta_1, \theta_2, \varphi_{12}) dr_{12} d\Omega$$

With

$$\int_\Omega d\Omega = \int_0^\pi S_1 d\theta_1 \int_0^\pi S_2 d\theta_2 \int_0^{2\pi} d\varphi_{12} .$$

Also,

$$e(r) = exp(-\phi/kT)$$

And

$$F(r_{12}, \theta_1, \theta_2, \varphi_{12}) = \left(\frac{\partial\varnothing}{\partial\theta_1}\right)^2 + \left(\frac{\partial\varnothing}{\partial\theta_2}\right)^2 + (csc^2\theta_1 + csc^2\theta_2 - 2)\left(\frac{\partial\varnothing}{\partial\varphi_{12}}\right)^2$$

$$-2\left(\frac{\partial\varnothing}{\partial\varphi_{12}}\right)S_{12}\left\{cot\theta_2\left(\frac{\partial\varnothing}{\partial\theta_1}\right) + cot\theta_1\left(\frac{\partial\varnothing}{\partial\theta_2}\right)\right\}$$

$$+2C_{12}\left\{\left(\frac{\partial\varnothing}{\partial\theta_1}\right)\left(\frac{\partial\varnothing}{\partial\theta_2}\right) - cot\theta_1 cot\theta_2 \left(\frac{\partial\varnothing}{\partial\varphi_{12}}\right)^2\right\}$$

In order to estimate the computational imprecision in C, the total number of partitions and the range of integration, r_{max}, were varied independently; as a result, it was estimated that at 200K, the numerical uncertainty was between 3 – 5 percent, however, this declined to about 1 percent at 400 K.

4. POTENTIAL PARAMETERS

The Maitland-Smith pair potential function has four parameters (ε/k, r_m, m, κ) and the values for ethane were determined in a fit to the experimental second acoustic virial coefficients of Estrada-Alexanders; no other data were used in the fit. The parameters were determined by solving the nonlinear least-squares problem:

$$\chi^2 = \mathbf{R}^T\mathbf{R} \quad (11)$$

Where,

$$R_i(\mathbf{X}) = (\beta_{i,cal} - \beta_{i,expt})/s_i\sqrt{N - N_p}$$

Here, $\mathbf{x}$ is the parameter vector, $\beta_{i,expt}$, is the value of the i-th experimental second acoustic virial coefficient, $\beta_{i,cal}$ is the corresponding value of the calculated second acoustic virial coefficient, N is the number of second acoustic virial coefficient data, N_p is the total number of adjustable parameters and s_i is the estimated standard deviation of $\beta_{i,expt}$. The following values minimized Eq. (11): ε/k = 592.453 K, r_m = 0.406519 nm, m= 16.785, κ = 12.0

Third virial coefficient data were not employed in the parameter optimization because of the excessive amount of computation that would have been required. Instead the value for the three-body strength coefficient of Eq. (6) was set equal to the value obtained in (Monago, 2010); namely, ϑ_{123}/k = 0.013901 K nm^9. Also, the quadrupole moment of ethane was assigned a value of $(\Theta/\sqrt{k})$ = 0.323 (K nm^5)$^{1/2}$ (Ameling et al., 1986) and the distance between the sites was set equal to the C—C bond length in ethane (0.1534 nm).

5. RESULTS AND DISCUSSION

Tables 1 and 2 contains the Second and third volumetric virial and acoustic virial coefficients of ethane respectively.

Table 1. Second and third volumetric virial coefficients of ethane

T/[K]	B/[cm^3/mol]	C/cm^6/mol^2]	T/[K]	B/[cm^3/mol]	C/cm^6/mol^2]
200	-420.28	-14617	305	-176.11	10093
210	-379.47	-4137	307	-173.7	10031
220	-344.73	2239	309	-171.34	9968
235	-301.11	7400	313	-166.74	9837
240	-288.43	8393	315	-164.5	9770
250	-288.50	9694	318	-161.21	9669
260	-244.94	10364	325	-153.87	9428
265	-235.58	10537	330	-148.89	9254
275	-218.35	10661	340	-139.52	8908
280	-210.40	10641	345	-135.1	8738
285	-202.85	10581	365	-119.06	8087
290	-195.72	10490	385	-105.19	7500
295	-188.83	10375	415	-87.59	6746
298	-184.89	10296	450	-70.8	6044
300.65	-181.50	10222	500	-51.83	5301
304	-177.33	10124			

Table 2. Second and third acoustic virial coefficients of ethane.

T/[K]	β/[cm^3/mol]	γ/cm^6/mol^2]	T/[K]	β/[cm^3/mol]	γ/cm^6/mol^2]
210	-501.98	26295	307	-242.02	27764
220	-459.19	30850	309	-238.88	27543
235	-405.09	33465	313	-232.76	27101
240	-389.24	33676	315	-229.77	26882
250	-360.26	33516	318	-225.38	26560
260	-334.37	32861	325	-215.51	25825
265	-322.44	32418	330	-208.77	25315
275	-300.33	31398	332	-206.15	25114
280	-290.06	30847	340	-196.02	24341
285	-280.27	30280	345	-189.97	23877
290	-270.91	29706	365	-167.73	21523
295	-261.97	29131	385	-148.16	20672
298	-256.79	28784	415	-122.81	18800
300.65	-252.32	28481	450	-97.98	17077
304	-246.82	28103	500	-69.14	15252
305	-245.2	27988			

Figure 1 compares experimental second volumetric virial coefficients with values determined in this work and it is clear that all the data lie within a band with an absolute deviation of 0.5 cm^3 mol^{-1}.
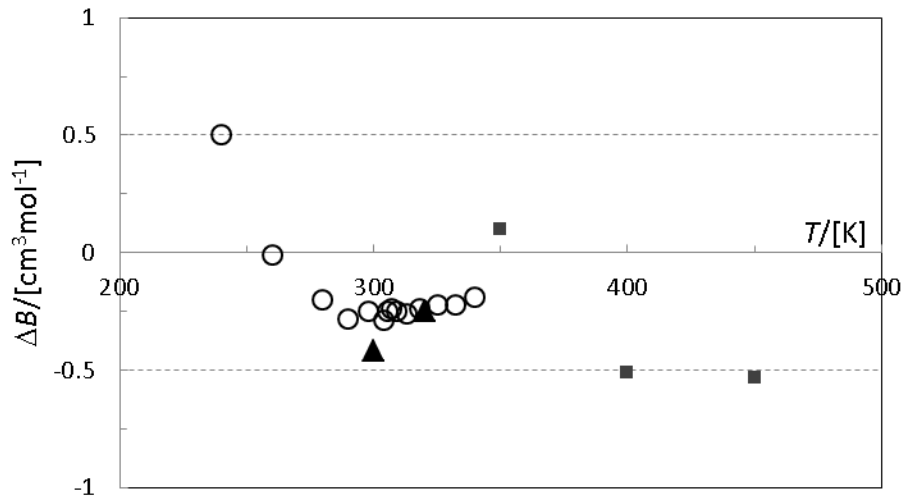
Figure 1. Deviations $\Delta B = B_{expt} - B_{cal}$ in experimental second volumetric virial coefficients of ethane from values calculated with the site-site model: $\circ$ ref. 16, $\blacktriangle$ ref. 17, $\blacksquare$ ref. 18

In Figure 2, experimental second acoustic virial coefficients are compared with values determined with the present model; here, we also find that most of the data lie within a band corresponding to an absolute deviation of 0.5 cm^3.
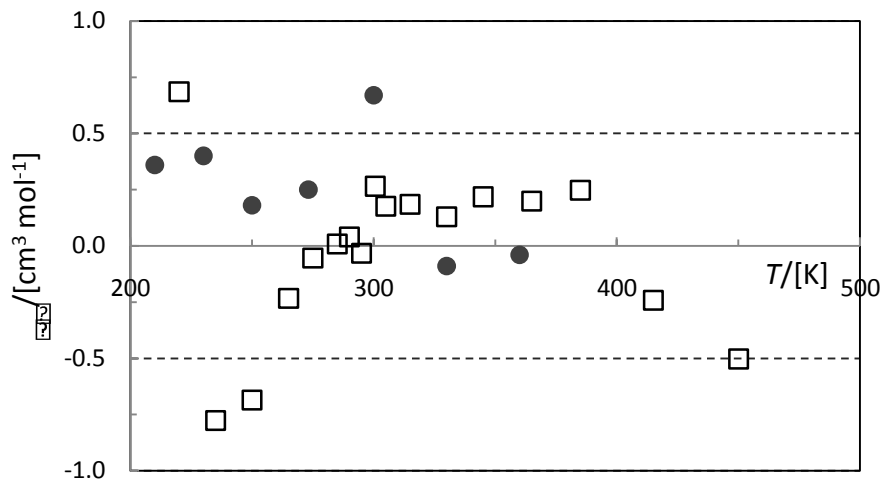
Figure 2. Deviations $\Delta\beta = \beta_{expt} - \beta_{cal}$ in experimental second acoustic virial coefficients of ethane from values calculated with the site-site model: $\square$ ref. 5; $\bullet$ ref. 19.

Figure 3 is a deviation plot of experimental third volumetric virial coefficients of ethane from calculated values, from which it is seen that most of the data lie within an absolute deviation of 250 cm^6 mol^{-2}.
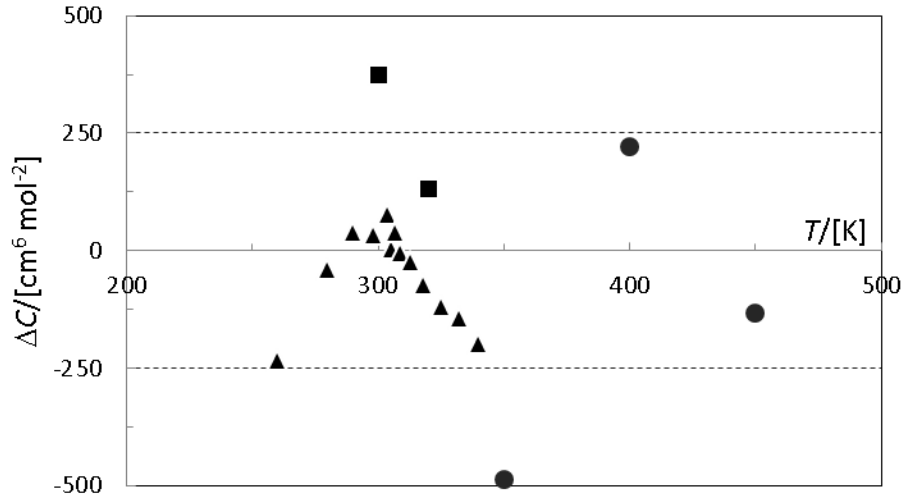
Figure 3. Deviations $\Delta C = C_{expt} - C_{cal}$ in experimental third volumetric virial coefficients of ethane from values calculated from the site-site model: ▲ ref. 16, ■ ref. 17, ● ref. 18.

In Figure 4 we display values of third volumetric virial coefficients of ethane as a function of temperature.
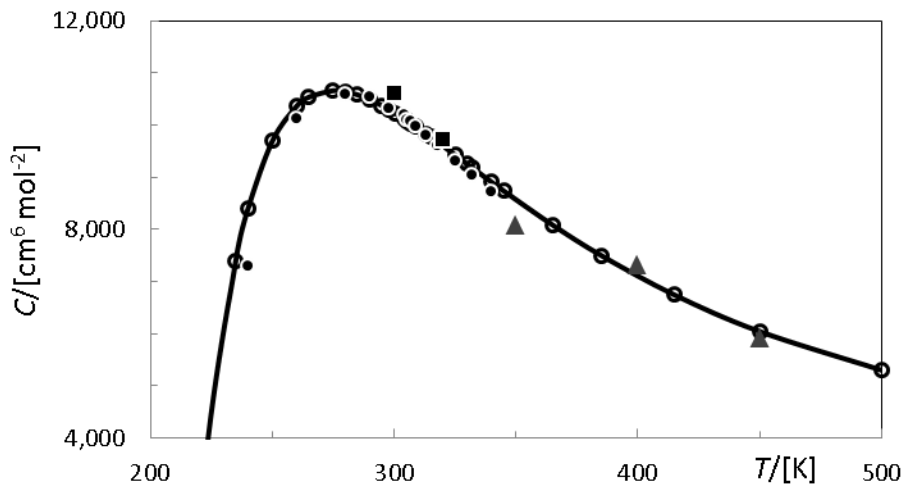
Figure 4. Third volumetric virial coefficient of ethane as a function of temperature: ● ref. 16, ■ ref. 17, ▲ ref. 18, ○&————, this work.

Figure 5 is a plot of third acoustic virial coefficients of ethane into which the experimental data of Estrada-Alexanders (1996) and those of Boyes (1992) have been inserted. The agreement in this case is not as good as was the case with the volumetric analogue; this is particularly so below a temperatureof 265 K for the data of Estrada-Alexanders and below 230 K for the data of Boyes.
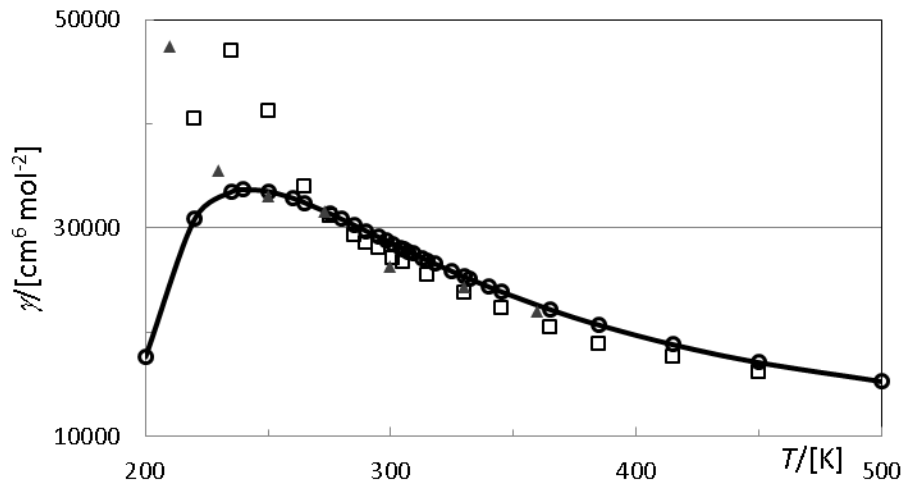
Figure 5. third acoustic virial coefficient of ethane as a function of temperature: ▢ ref. 5, ▲ ref. 19; ○& —————, this work.

6. CONCLUSION

Calculation of third virial coefficients of linear molecules with a site-site pair potential is computationally demanding; particularly if one should desire to fit potential parameters to experimental data. In this paper site-site two-body potential parameters were determined in a fit to second acoustic virial coefficients alone, while the three-body strength coefficient was determined in a fit to acoustic data using isotropic two-body and three-body potential models. It is shown that when the site-site potential is combined with the Axilrod-Teller triple-dipole term, the procedure predicted second and third volumetric virial coefficients that are in agreement with the most precise experimental data available. The calculations in this paper lend support to the fact that available experimental third acoustic virial coefficients of ethane might be inconsistent with the volumetric counterpart at temperatures below 240 K.

REFERENCES

Ameling, W. and Lucas K. (1986). Correlation and extrapolation of dilute-gas properties of simple linear molecules with the SSR-MPA potential model, International Journal of Thermophys 7, 1135 -1145.

Ameling, W., Shukla,K. .P and Lucas, K. (1986). Third virial coefficient of simple linear molecules, Mol. Phys 58, 381-394.

Benjamin, K.M., Schultz, A.J. and Kofke, D.A. (2009). Fourth and fifth virial coefficients of polarizable water, Journal of Phys. Chem. B, 113, 7810.

Boyes, S.J. (1992). The speed of sound in gases with applications to equations of state and sonic nozzles, Ph.D. thesis, University of London, London, U K.

Crisancho, D.E., Mantilla I.D., Ejaz, S., Hall, K.R., Atilhan, M. and Iglesias-Silva, G.A., (2010). Accurate PρT data for ethane from (298 to 450) K up to 200 MPa, Journal of Chem. Eng. Data 55, 2746-2749.

Estela-Uribe, J.F. and Trusler, J.P.M. (2000). Acoustic and volumetric virial coefficients of nitrogen, International Journal Thermophys 21, 1033-1044.

Estrada-Alexanders, A.F. (1996). Thermodynamic properties of gases from measurements of the speed of sound, Ph. D. Thesis, University of London, London, U K.

Ewing, M.B. and Trusler, J.P.M. (1992). Second acoustic virial coefficients of nitrogen between 80 and 373 K, Physica A, 184, 415-436.

Funke, M., Kleinraham, R. and Wagner, W. (2002). Measurement and correlation of the (P, ρ, T) relation of ethane Journal of Chem. Thermodyn 34, 2001-2015.

Hou, H., Holste, J.C., Hall, K.R., Marsh, K. N. and Gammon, B.E. (1996). Second and third virial coefficients for methane+ethane and methane+ethane+carbon dioxide at (300 and 320) K,   Journal of Chem. Eng. Data 41, 344-353.

Kim, H.M., Schultz, A.J. and Kofke, D.A. (2013). Second through fifth virial coefficients for model methane-ethane mixtures, FluidPhaseEquilibria, 351, 69-73.

Kusalik, P.G., Liden, F.L. and Svishcher, I. M. (1995). Calculation of the third virial coefficient for water,Journal of Chem. Phys 103, 10169-10175.

Lucas, K. (1991). Applied Statistical Thermodynamics, (Springer-Verlag, Berlin) 284 – 286.

Meng, L. and Duaa, Y.Y. (2006). Site-site potential function and second virial coefficients for linear molecules, Mol. Phys., 104, 2891- 2899.

Monago, K.O. (2005). An equation of state for gaseous argon determined from the speed of sound Chem. Phys 316, 5 – 9.

Monago, K.O. (2010). Equation of state for gaseous ethane determined from isotropic model potentialsKorean Journal of Chem. Eng 27, 590 – 595.

Monago, K.O. (2013). Comments on 'on an equation of state for gaseous argon determined from the speed of sound'Chem. Phys 441, 45 – 48.

Pack, R. T. (1983). First quantum corrections to second virial coefficients for anisotropic interactions: simple corrected formulas, Journal of Chem. Phys 78, 7217 – 7222.

Shaul, K.R.S., Shultz, A.J. and Kofke, D.A. (2011). Mayer sampling Monte Carlo calculations of uniquely flexible contributions to virial coefficients, Journal of Chem. Phys 135.

Wiebke, J., Scherdtfeger, P., Moyano, G.E., and Pahl, E. (2011). An atomistic fourth-order virial equation of state for argon from first principles calculationChem. Phys. Lett 514, 164 – 167.